PROPERTY ESTIMATION OF A 2D CARBON FIBER PREFORM: FOR THE SIMULATION OF ICVI PROCESSES

*Aijun Li, Günter Schoch, Sven Lichtenberg, Olaf Deutschmann**
Institut für Technische Chemie und Polymechemie, Universität Karlsruhe, 76131 Karlsruhe, Germany

Abstract:

Porosity properties of a 2D carbon fiber preform with a 0/0/90/90° fiber architecture and an overall fiber volume fraction of 22.5% were investigated in order to provide enough information for the simulation of ICVI processes of pyrolytic carbon from methane. An initial porosity of 92.9% was assumed for the sub-layer of randomly distributed fibers of the 2D carbon fiber preform and 67.4% for the sub-layer of parallel fibers. Both theoretical calculation and simulation of porous structure evolution are performed, such as overall surface area and equivalent radius of pores as a function of porosity. These properties were employed to simulate the densification process of the 2D carbon fiber preform, based on the multi-step deposition model and the hydrogen inhibition model. Corresponding experimental conditions were temperature of 1070, 1095 and 1100°C and pressures of 12.5-32.5kPa of methane. Acceptable agreement of bulk density was achieved between the predicted and experimental results in reference. Conditions for achieving homogeneous densification are also predicted.

Key words: Carbon composites, Chemical vapour infiltration, Pyrolytic carbon

1. Introduction

Methods of deposition of solid phases on inner surface of porous medium by decomposition of volatile or gaseous compounds which contain the solid phase elements are designated as chemical vapor infiltration (CVI) [1,2]. CVI are of importance with respect to the fabrication of refractory materials which normally possess low density but exhibit very nice mechanical properties and noncatastrophic failure required in many high-temperature aerospace and energy application [3]. However, CVI is an extremely complex process, in which there is a particular problem that the volatile or gaseous precursor must be transported through pores into the interior of porous preforms and forms matrix by chemical vapor deposition before its dissolving on the external surface. Generally, there are four primary subprocesses in CVI, namely homogeneous gaseous reactions, heterogeneous surface reactions, and mass heat transfer as well as heat transfer. Therefore, their interaction controls the densification mode of porous preforms as well as the microstructures (textures) of deposit. Concerning various embodiments of CVI for production of carbon/carbon composites, different subprocess dominates the process. As the simplest method widely used in industry, isobaric and isothermic CVI (ICVI) leads to products with very good mechanical properties and can produce objects with complex shape and large size, while ICVI is a diffusion driven and mass transfer limited process. Thereby, the most serious disadvantage of ICVI lies in being a slow and, as a result, expensive process [3].

Fiber architectures of preforms are the backbone of as-obtained composites, determining the properties of the composites. Carbon felt of discretely distributed fibers is easily processed and has nearly homogeneous three-dimensional structure, however its fiber volume fraction and strength translation efficiency in composites made of discrete fibers are quite low. To overcome the above problem, unidirectional preforms of parallel carbon fibers theoretically possessing the highest fiber packing efficiency has the highest level of properties translation efficiency. However, this kind of preform is widely used only for basic research because as-obtained composites are particularly poor in out-of-plane strength [4]. Combining advantages of both preforms, 2D carbon fiber felts which possess a special "0/0/90/90°" architecture described in details in Ref. [5] are normally used as the preforms of C/C composite brake disks. Evolution of pore geometries of 2D carbon fiber felts such as surface area and equivalent radius of pores are investigated and these results are then employed to simulate densification of this kind of preform by ICVI processes based on the multi-step deposition model and the hydrogen inhibition model [6, 7]. Predictions of bulk density distribution and the effect of pressures and temperatures on densification are compared with experimental data.

* Corresponding author.Tel.: +49-721-608-3138; fax: +49-721-608-4805
Email: deutschmann@ict.uni-karlsruhe.de (O. Deutschmann), li@ict.uni-karlsruhe.de (A. Li)

2. Modeling approach

2.1 Evolution of pore geometries of 2D carbon fiber felts

As illustrated in Fig.1, there are two types of sublayers, i.e. the layers of oriented fibers (unidirectional, 2/4) and the layer of randomly distributed fibers (discrete, 1/3/5) in the 2D carbon fiber felts used in the present work. OA and O'A' are two periodic boundaries. The overall fiber volume fraction of the 2D carbon fiber felt is 22.5%. An initial porosity of 92.9% was assumed for the sublayer of randomly distributed fibers and 67.4% for the sublayer of oriented fibers. According to the principle of evolution of porosity, the following equations can be deduced if we assume concentration distribution is homogeneous in the small domain of Fig.1.

$$\frac{d\varepsilon_1}{S_{V_1}} = \frac{d\varepsilon_2}{S_{V_2}} \tag{1}$$

where ε_1 and ε_2 define porosities of the randomly distributed fiber layer (Layer1) and the oriented fiber layer of (Layer2), respectively. S_{V_1} and S_{V_2} represent the surface area of each layer. Up to now, several laws of surface area have been developed to describe the evolution behaviors of surface area versus porosity [8, 9]. In the present work, two surface area models have been tested, as shown in eqns (2) and (3).

$$S_V = \frac{2}{r_f}\sqrt{\frac{1-\varepsilon_o}{\varepsilon_o}}\sqrt{(1-\varepsilon)\varepsilon} \tag{2}$$

$$S_V = \frac{2}{r_f}\frac{\varepsilon}{\varepsilon_o^2}(1-\varepsilon)(\varepsilon_o + \ln\varepsilon_o - \ln\varepsilon) \tag{3}$$

where r_f and ε_o define the initial radius of fibers and the initial porosity, respectively. For theoretical calculations of the overall surface area profile of 2D carbon fiber felts, eqn (2) was employed, which was proposed according to totally different evolution behaviors of surface area corresponding to very low and to very high porosity, respectively.

If S_{V_o} is defined as follows:

$$S_{V_o} = \frac{2}{r_f}\sqrt{\frac{1-\varepsilon_o}{\varepsilon_o}} \tag{4}$$

Combining eqns (1), (2) and (4), then gives:

$$\frac{d\varepsilon_1}{S_{V_{1o}}\sqrt{(1-\varepsilon_1)\varepsilon_1}} = \frac{d\varepsilon_2}{S_{V_{2o}}\sqrt{(1-\varepsilon_2)\varepsilon_2}} \tag{5}$$

Then:

$$\arcsin\sqrt{\varepsilon_1} - \arcsin\sqrt{\varepsilon_{1o}} = \frac{S_{V_{1o}}}{S_{V_{2o}}}\left(\arcsin\sqrt{\varepsilon_2} - \arcsin\sqrt{\varepsilon_{2o}}\right) \tag{6}$$

Obviously, Layer1 exhibits a much lower fiber volume fraction and thus a much lower surface area compared to that of Layer2, resulting in a higher densification rate in layer2. Therefore Layer2 will be well densified first and after then densification will exist only in Layer1. Taking into account some closed porosity (about 5% porosity remaining after densification), the porosity of Layer1 when Layer2 is densified well can be calculated as follows:

$$\varepsilon_1\Big|_{\varepsilon_2=0.05\varepsilon_{2o}}^{t:} = \sin^2\left[\arcsin\sqrt{\varepsilon_{1o}} + \frac{S_{V_{1o}}}{S_{V_{2o}}}\left(\arcsin\sqrt{0.05\varepsilon_{2o}} - \arcsin\sqrt{\varepsilon_{2o}}\right)\right] \tag{7}$$

Considering the volume fraction of each sublayer, the overall porosity of 2D carbon fiber felt at this moment is:

$$\varepsilon = \frac{1.7}{4.3}\varepsilon_1\Big|_{\varepsilon_2=0.05\varepsilon_{2o}}^{t:} + 0.05\varepsilon_{2o}\frac{2.6}{4.3} \tag{8}$$

Once the key value is figured out, the densification process may be divided into two stages. The first stage is corresponding to densification process at two different layers of which the porosities decrease by eqn (2, 6) and the second stage to the densification of Layer2. Fig.2a shows the theoretical profile of the overall surface area versus overall porosity of 2D carbon fiber felt. If eqn (2) is used directly to calculate the overall surface area versus overall porosity of 2D carbon fiber felt without consideration of the distinction of different sublayers, the profile will be dramatically changed (the dash line shown in Fig. 2a).

Provided that mean radius of pores of 2D carbon fiber felt is $\bar{r}$ and standard deviation of pore radius distribution is σ, the following equation between surface area and porosity exists:

$$S_V = \frac{1}{1+(\frac{\sigma}{\bar{r}})^2}\frac{2\varepsilon}{\bar{r}} \quad (9)$$

Measurement of pore radius distribution shows that for carbon fiber felts of 92.9% porosity, the normal value of standard deviation σ is less than $10\,\mu m$. Mean radius $\bar{r}$ reduces normally from about 50 to $1\,\mu m$ with progressive densification [10]. Therefore, pore radius distribution has very little influence on surface area except in the last stage of densification. Since some closed porosity exists in the last stage of densification, pore radius distribution also has no substantial effect on surface area and surface. So in the present work, a homogeneous distribution of pore radius is assumed, which results in a simplified eqn.(8).

$$\bar{r} = \frac{2\varepsilon}{S_V} \quad (10)$$

Fig.2b illustrates theoretical profiles of the overall equivalent pore radius of 2D carbon fiber felts. It is worthy of note that surface area decreases dramatically once the oriented fiber layer is well densified first, while it has seldom adverse effect on mass transport of precursor because equivalent pore radius only decreases a little bit. Therefore the advantage of 2D carbon fiber felt is that the randomly distributed fiber layer acts as a transport channel for the diffusion of the gas into the preform during the densification, especially after the oriented fiber layer is well densified [5].

Due to the difficulty of the integration of eqn (3), a theoretical calculation of the overall surface area is impossible. Therefore FEM calculations are carried out by use of the representative volume element as shown in Fig.1. A fictitious first-order densification of was assumed on the basis of the following mass balance equation (or equivalently, the solid phase) given in terms of the pore space.

$$CH \xrightarrow{k_1} C + 0.5H_2 \quad (11)$$

$$\frac{d\varepsilon}{dt} = -V_C k_{CH} c_{CH} \frac{2}{r_f}\frac{\varepsilon}{\varepsilon_o^2}(1-\varepsilon)(\varepsilon_o + \ln\varepsilon_o - \ln\varepsilon) \quad (12)$$

where, V_C is the molar volume of carbon deposit and normally, its value is from 5.5 to 8 (10^{-6}m^3 mol^{-1}). k_{CH} defines the surface reaction rate constant of the fictitious first-order densification. Assuming concentration is constant, a fictitious value of $V_C k_{CH} c_{CH}$ was set to be 1 (10^{-6}m s^{-1}) in the present work.

Simulation can be easily carried out by using any FEM software and COMSOL3.1 was employed in this present work. Predicted results of the overall surface area and the equivalent radius of pores are shown in Fig.2a and 2b. It is clear eqns (2) and (3) exhibit different evolution profiles of surface area and equivalent radius.

2.2 Transient simulation of ICVI from methane of 2D carbon fiber felts

A lot of work has been devoted to develop or employ mathematical and physical models such as dusty gas model and Darcy's law in order to describe the dynamic behavior of CVI processes [3]. Simulation results of Vignoles and co-workers show that relative difference on porosity is less than 1% if viscous flow resulting from pressure gradient is ignored in film-boiling CVI processes (a kind of thermal gradient CVI). In the current work, ICVI exhibiting very low pressure and thermal gradients is used to produce C/C composites. Therefore, only mass transport by diffusion is taken into account, as follows.

$$\frac{d(\varepsilon c_i)}{dt} + \nabla \cdot J_i = \varepsilon R_{ig} + R_{is} \quad (13)$$

where, c_i defines the concentration of ith gaseous species and J_i is the effective diffusion flux of the species. R_{ig} and R_{is} are the overall rate of all homogeneous gaseous reactions involving ith species and the heterogeneous surface reaction of ith species, respectively.

Methane is used as the precursor of carbon in the present work. To give deep insight into the effect of chemical reactions on CVI processes of methane, the multi-step deposition model and hydrogen inhibition model were developed [6, 7]. Generally, maturation of gaseous composition begins with decomposition of methane and carbon deposition was controlled by several dominating gaseous species, i.e. ethylene, acetylene and benzene, while hydrogen has very strong inhibition effect on carbon deposition depending on the concentration ratio of hydrogen to hydrocarbons. Carbon deposition directly from methane is impossible but small amount of carbon deposition was found by extrapolation corresponding to zero residence time [11], which may result from either pre-decomposition of methane or carbon formation from other C_1 species such as methyl. Therefore this possible contribution to carbon formation is involved by counting carbon deposition from methane at few percent of original measured reaction rate. According to these models, the balance equation of porosity is given by

$$\frac{d\varepsilon}{dt} = -V_C \sum_i \nu_{is} R_{is} \quad (14)$$

where ν_{is} is the stoichiometric coefficient of the carbon deposition reaction of ith species and R_{is} can be written as

$$R_{is} = S_v k_{is} I_{is} c_i \quad (15)$$

where k_{is} is the rate constant of carbon deposition from ith species and I_{is} is the inhibition function of ith species. Details of these parameters have been given in our past paper [7]. Provided that densities of pyrolytic carbon and carbon fiber are ρ_C and ρ_f respectively, bulk density of C/C composites (ρ) can be written as

$$\rho = \varepsilon_o \rho_f + (\varepsilon - \varepsilon_o)\rho_C$$

Transient simulations of ICVI are performed using porous structure evolution models shown in Fig.2 with the FEM platform of COMSOL3.1. Corresponding experimental setup and geometrical model of the CVI reactor are described in details in Ref. [5] and [7].

3. Results and discussion

3.1 Bulk density

Predicted and experimental bulk densities versus infiltration time are illustrated in Fig.3. It is worthy of note that simulation result employing eqn (2) exhibits lower densification rate and then much difference to the experimental data, while eqn (3) leads to a sound prediction of densification. In the following sections, simulations are all based on eqn (3). The maximum error is about 8% between experimental data and the predicted employing eqn (3). The error maybe derives from several possibilities. Before making measurement of bulk density, a thickness of 1-1.5mm round about was always cut off from surface of the as-obtained C/C composites, which will affect the measured value a little bit. However, this operation is not included in our simulation. Another possibility maybe comes from the current chemical model. In gas phase, there should not be only one route for the formation of important intermediate gaseous species. For example, there are at least two routes for the formation of benzene from C_2 species, i.e. C_3 and C_4 routes [12]. Which route is the dominating one depends on reaction conditions such as temperature, pressure and surface area. Surface reactions will consume a lot of intermediate products of gas phase reactions, which probably leads to either a shift of the current dominating route to another one or at least variations of overall kinetic data of the multi-step deposition model. The current chemical reaction model was developed for ICVI of carbon fiber felts, while 2D carbon fiber felts exhibiting totally different surface area are employed in the present. Moreover, hydrogen inhibition functions were derived by experimental data at a given temperature (1000°C) and it is not validated in a wide rage of temperatures.

It is also worthy of note that much difference between the surface area profile of eqn(2) and eqn(3) does not lead to the same level difference between bulk density profiles. It is seen that the gradient of the equivalent radius of pore of eqn(3) is larger than that of eqn(3) as shown in Fig.2b. Compared with eqn(3), poor effect of the lower surface area of eqn(2) on carbon deposition rate is compensated by the higher mass transport capability due to its larger equivalent radius of pores.

3.2 Influence of pressure and temperature on bulk density distribution

The influence of pressure of methane on bulk density distribution is investigated by simulations illustrated in Fig.4. Inside to outside densification is achieved when pressure is lower than 25kPa that is similar with experimental result [5]. Higher pressure than this value will lead to a higher overall deposition rate on the surface than inside the porous perform, and then the pores of surface easily become clogged. Fig.5 presents the effect of temperature on density distribution. Decreasing temperature or pressure is helpful to obtain inside to outside densification. Homogeneous densification conditions are 20kPa at 1100°C and 25kPa at 1095°C. However, homogeneous densification at 1070°C can not be achieved up to 30kPa as shown in Fig.5.

4. Summary

In the present work, evolution properties of 2D carbon fiber felts such as the overall surface area and the equivalent radius of pores are evaluated by use of two different models. The structural advantage of 2D carbon fiber felt is numerically proven that the randomly distributed fiber layer acts as a transport channel for the diffusion of the gas into the preform during the densification, especially after the oriented fiber layer is well densified. The predicted evolution properties are employed to simulate densification of the 2D carbon fiber felt by ICVI. A sound agreement between experimental and predicted profiles of bulk density versus time is obtained. It is worthy of note that the effects of perform anisotropy on densification processes must be considered in simulations. The influences of temperature and pressure on bulk density distribution are also investigated. Homogeneous densification conditions are predicted by simulations.

Reference

[1]. Savage G. Carbon-carbon composites, Chapman & Hall, London; 1992.

[2]. Kotlenski W. Deposition of pyrolytic carbon in porous solids. In: Walker Jr. PL, Thrower PA, editors, Chemistry and physics of carbon, New York: Marcel Dekker, 1973, 9: 173-262

[3]. Sotirchos S. Dynamic modeling of chemical vapor infiltration, AIChE Journal, 1991, 37(9): 1365-1378.

[4]. Fitzer E, Manocha LM. Carbon reinforcements and carbon/carbon composites, Berlin, Heidelberg: Springer, 1998: 190-236.

[5]. Zhang WG, Hüttinger KJ. Densification of a 2D carbon fiber preform by isothermal, isobaric CVI: Kinetics and carbon microstructure, Carbon 2003(41): 2325–2337

[6]. Li, HJ, Li, AJ, Bai, RC, Li, KZ. Numerical simulation of chemical vapor infiltration of propylene into C/C composites with reduced multi-step kinetic models. Carbon 2005(43), 2937–2950.

[7]. Li AJ, Deutschmann O. Transient modeling of chemical vapor infiltration of methane using multi-step reaction and deposition models. Chemical Engineering Science, 2007, in press.

[8]. Vignoles, G.L., Goyhénèche, J.-M., Sébastian, P., Puiggali, J.-R., Lines, J.-F., Lachaud, J., Delhaès, P., Trinquecoste, M., 2006. The film-boiling densification process for C/C composite fabrication: from local scale to overall optimization. Chemical Engineering Science 61, 5336-5353

[9]. Vaidyaraman S, Lackey WJ, Starr TL. 1-D model for forced flow-thermal gradient chemical vapor infiltration process for carbon/carbon composites. Carbon 1996;34(9):1123−1133.

[10]. Li AJ, Norinaga K, Zhang WG, Deutschmann O. Modelling and simulation of materials synthesis: chemical vapor deposition and infiltration of pyrolytic carbon. Composite Science and Technology, submitted.

[11]. Bruggert M, Hu Z, Hüttinger KJ. Chemistry and kinetics of chemical vapor deposition of pyrocarbon VI. influence of temperature using methane as a carbon source. Carbon 1999, 37: 2021– 2030

[12]. Li AJ, Schoch G, Lichtenberg S, Zhang D, Deutschmann O. A novel CVD/CVI reactor with an in situ sampling apparatus connected to an online GC/MS. Surface and Coatings Technology, 2007, in press.

Fig.1 Illustration of 2D carbon fiber felts (2/4: the layers of oriented fibers. 1/3/5: the layer of randomly distributed fibers)

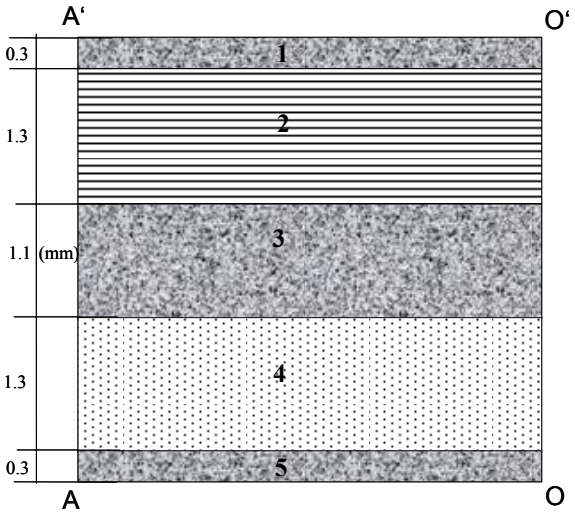

Fig.2 Profiles of surface area and equivalent pore radius of 2D carbon fiber felts

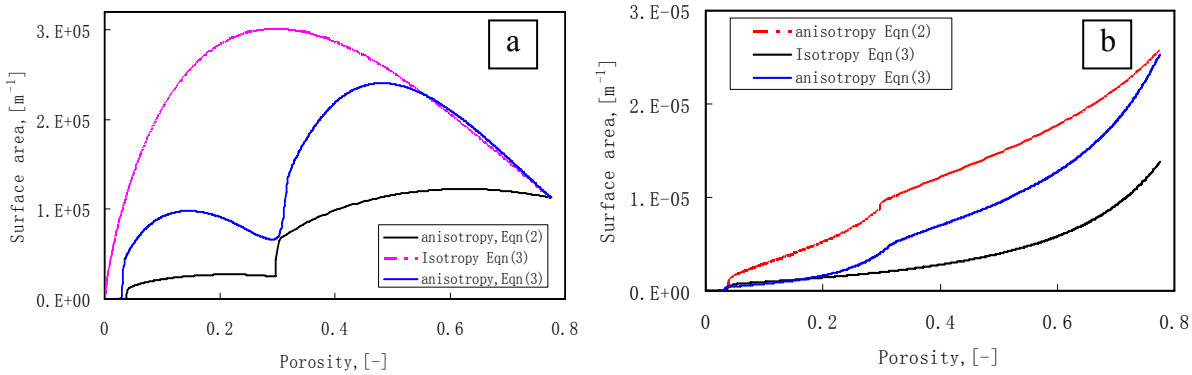

Fig.3 Densification profile of 2D carbon fiber felts versus infiltration time at a temperature of 1095°C and pressure of methane of 22.5kPa.

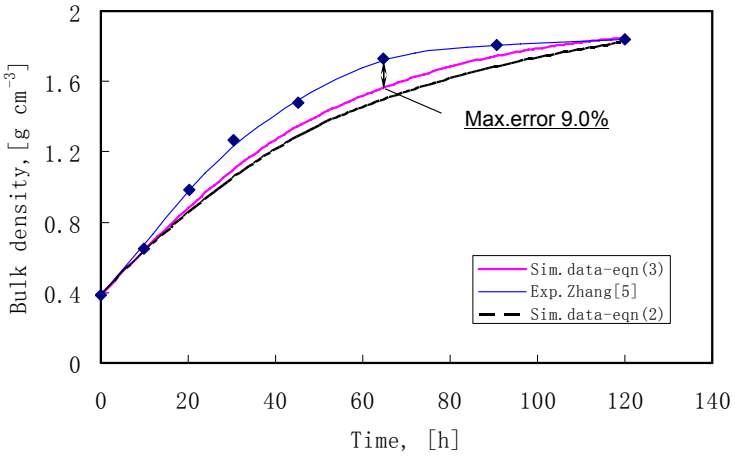

Fig.4 Prediction on the influence of pressures on bulk density distribution at a temperature of 1095°C (120h densification)

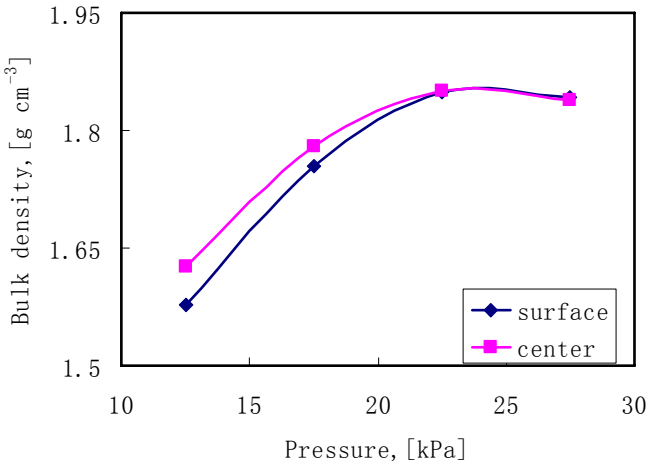

Fig.5 Prediction on the influence of temperatures on bulk density distribution (120h densification)